

# SiO Maser Dependency on the Circumstellar Shell of AGB Stars

by

**Stephanie Hansen**

**B.S. Astrophysics**

**(Physics and Astronomy, University of New Mexico, 2023)**

## **ABSTRACT**

Stars on the Asymptotic Giant Branch (AGB) are of low to intermediate mass and have reached the end stages of stellar evolution. These stars become encompassed by a circumstellar envelope (CSE) that redistributes the stellar light into the infrared (IR) regime. In these envelopes, molecules such as SiO can form and create maser emission at radio frequencies. The Bulge Asymmetries and Dynamical Evolution (BAaDE) survey observes SiO emission in thousands of Galactic AGB stars near the central region of the Milky Way. In this paper I am expanding that survey to explore possible correlations between the radio emission of the SiO masers and the IR emission of the circumstellar envelope.

# TABLE OF CONTENTS

|          |   |           |
|----------|---|-----------|
| <b>1</b> | <b>Introduction</b>                       | <b>1</b>  |
| 1.1      | SiO Masers in the Asymptotic Giant Branch | 1         |
| 1.2      | The Original BAaDE Data                   | 3         |
| 1.3      | Extending the Color Range                 | 4         |
| <b>2</b> | <b>Infrared Catalog Building</b>          | <b>5</b>  |
| 2.1      | IR Coverage Overview                      | 5         |
| 2.2      | Finding 2MASS Positions                   | 5         |
| 2.3      | Photometry Filtering                      | 7         |
| 2.4      | 2MASS Cases with Multiple Candidates      | 8         |
| 2.5      | Other Catalogs with Multiple Candidates   | 9         |
| 2.6      | Cross-Match Confirmation with 2MASS       | 10        |
| <b>3</b> | <b>Radio Data</b>                         | <b>10</b> |
| 3.1      | Observations with the Very Large Array    | 10        |
| 3.1.1    | Data Reduction                            | 12        |
| 3.2      | Results                                   | 14        |
| <b>4</b> | <b>Discussion</b>                         | <b>16</b> |
| 4.1      | Overall detection trends                  | 16        |
| 4.2      | Line Ratios Versus Infrared Color         | 16        |
| <b>5</b> | <b>Future Work</b>                        | <b>19</b> |
| <b>6</b> | <b>Conclusion</b>                         | <b>22</b> |
| <b>7</b> | <b>Acknowledgements</b>                   | <b>22</b> |

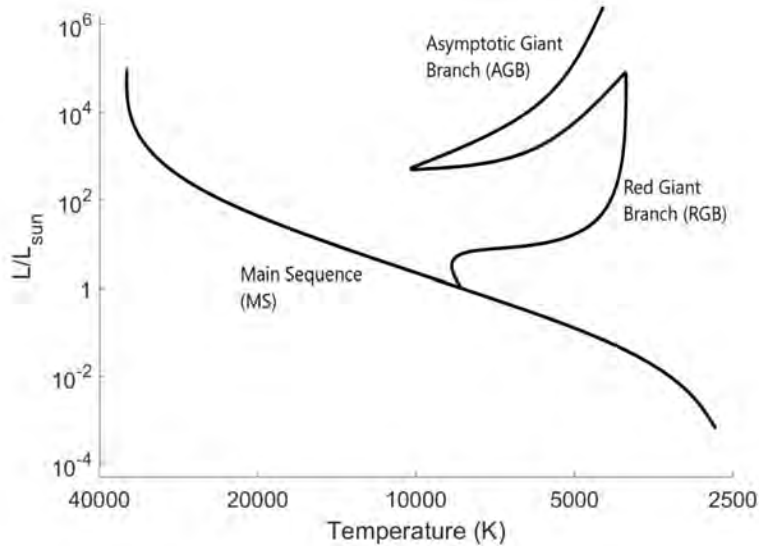


Figure 1: An HR Diagram highlighting the evolutionary path of low mass stars, below approximately  $6 M_{\odot}$ . The low temperatures and large sizes give these stars the common name of Red Giants. The BAaDE Survey targets these AGB stars.

## 1 Introduction

### 1.1 SiO Masers in the Asymptotic Giant Branch

Silicon Oxide (SiO) masers are formed when intermediate mass ( $1$  to  $5 M_{\odot}$ ) stars are in the last phase of the AGB stage. In a short span of time the star throws off most of its envelope, surrounding itself with a dense, circumstellar shell. As the envelope cools, dust particles form and obscure the central star. Those dust particles convert the stellar radiation into infrared photons (Habing, 2016), making AGB stars amongst the brightest IR emitters on the sky. Masers form when molecules (such as SiO) are “pumped up” from a lower energy level into a higher, long-lived metastable energy state. The molecule then makes a downward transition back to a lower state when it is stimulated by a photon with an energy equal to the difference in energies between the two states. The original photon and the emitted photon together amplify the radiation, causing the laser-like radio emission we observe.

We can observe this amplified radiation through spectral lines in the radio and millimeter

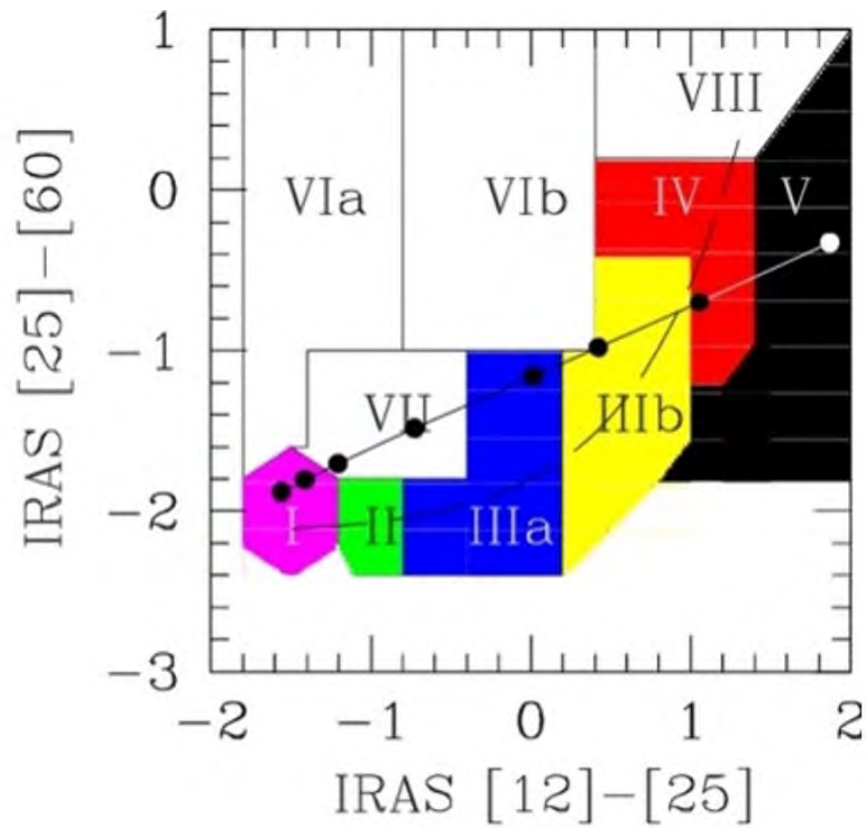


Figure 2: Color-color diagram used to choose targets for expanded range. The new IR catalog includes targets from ii and iiib.

regimes. The Doppler shift of the lines provide the line-of-sight velocity. Both line brightness and line ratios of the spectral lines inform about density and temperature of the gas. How much material that is being ejected depends on the metallicity of the star, the initial mass and effective temperature. The shell contains both dust and gas with the thickness of the shell determining the redness of its color. As the AGB stars continue to shed material, the dust envelope grows thicker and thus the emission gets redder. By studying details of the infrared emission, we can therefore learn about the composition and thickness of the circumstellar shell envelope (CSE). When coupled together, we expect to see some correlations between the spectral line properties from radio emission of the masers (line ratios, line strengths) and the infrared emission properties (brightness, colors, etc.) as discussed further in Section 4.

## 1.2 The Original BAaDE Data

Despite calling it home, studying and understanding the Milky Way, and especially the central bulge, has been a challenge, particularly due to our location in the disk. The material in the 8 kpc between us and the center of the bulge attenuates much of the visible light, requiring us to use longer wavelengths to study the structure and kinematics of the bulge and bar. Fortunately, there are plenty of stars that we can observe in the radio regime via molecular line transitions that we can then use to derive velocities to be used for studying the dynamics of the central region of the Milky Way. The BAaDE (Bulge Asymmetries and Dynamical Evolution) survey is a project which aims to measure line-of-sight velocities to evolved stars in the Milky Way disk and bulge region using radio data. The ultimate goal of the survey is to improve our models of the gravitational potential in the central region of the Milky Way. BAaDE has also built an extensive database of infrared photometry data of evolved stars in this region. To date, the BAaDE sample is the largest and most uniform database of SiO masers, making it the most comprehensive set of observations with which to compare SiO maser modeling. In the original BAaDE survey, over 9800 Galactic SiO masers have been identified using VLA observations, and over 1000 with ALMA so far, with 16000

expected once the data reduction is complete (Stroh *et al.*, 2019).

The exact properties of the SiO maser emission, in particular line ratios between various transitions, might be expected to vary as a function of CSE properties as measured by IR color. Initial work on this was made by Lewis *et al.*(2021), who found only a very weak trend as a function of color for the brightness ratio of the  $v=1/v=2$  transitions for the iiiia BAaDE sources observed by the VLA. Lewis’s results disagreed with results from 2007 (Nakashima & Deguchi, 2007) which found stronger correlations though with only 75 redder sources.

### 1.3 Extending the Color Range

There may be several reasons why it was hard to discern trends between the IR and spectral line properties, for example, the stars are variable which makes the infrared properties to be less well defined and lead to large uncertainties as not all IR data is collected simultaneously. This effect, coupled with a narrow range of colors initially used for the selected sample will make it harder to see correlations. This has been addressed by extending the color range of the sources used to search for correlations. The original survey used targets from the iiiia region in Figure 2, and now we are expanding to both bluer and redder sources in ii and iiib. Table 1 shows the color values that were used to choose the sources from the Midcourse Space Experiment (MSX) catalog, with those color values remapped from the IRAS colors shown in Figure 2.

To begin analyzing the sources of this extended color range, I collected infrared data for 8623 sources (3384 ii sources and 5239 iiib sources) from these extended color regions using existing databases and compiled them into one catalog for use by the BAaDE team. This work extended the database for the original work done on the 28,000 BAaDE sources in region iiiia by Eddie Hilburn (Hilburn, 2018). Then, I reduced observational data by the Very Large Array (VLA) to study the spectral line properties of 503 of these additional sources and look for possible correlations with the IR emission.

|            |  |    |  |    |                               |
|------------|--|----|--|----|-------------------------------|
| MSX ii:    | $-0.9 \leq [A] - [D] < -0.6$   | or | $-1.5 \leq [A] - [E] < -0.7$   | or | $-1.1 \leq [C] - [E] < -0.75$ |
| MSX iiiia: | $-0.6 \leq [A] - [D] < +0.4$   | or | $-0.7 \leq [A] - [E] < +0.4$   | or | $-0.75 \leq [C] - [E] < +0.1$ |
| MSX iiib:  | $+0.4 \leq [A] - [D] < +5.0$<br>and<br>$+0.1 \leq [C] - [E] < +0.55$ | or | $+1.4 * ([A] - [E]) - ([A] - [D]) < +0.8$<br>and<br>$+0.4 \leq [A] - [E] < +1.1$ | or | $+0.1 \leq [C] - [E] < +0.55$ |

Table 1: MSX color region boundaries used to choose sources for the BAaDE survey. Region iiiia is the original survey, region ii and iiib were used to extend the color range (Sjouwerman *et al.*, 2009)

## 2 Infrared Catalog Building

### 2.1 IR Coverage Overview

To be able to compare line ratios and infrared data, a database was constructed for all the 8623 sources belonging to the ii and iiib regions. Nine different catalogs were used for our database covering wavebands from 0.81 - 70  $\mu\text{m}$  (Table 2). We note that the IR data is a compilation of magnitudes from different sensitivities as well as sky coverages. Therefore, not all of our targets have data in all bands listed in Table 2.

All the catalogs but ISOGAL were accessed through the NASA/IPAC Infrared Science Archive (<https://irsa.ipac.caltech.edu>).

ISOGAL was accessed through the Vizier database (<https://vizier.cds.unistra.fr/viz-bin/VizieR>). In the following sections we describe how the data was collected through initial positional cross-matching followed by filtering to remove false cross-matches.

### 2.2 Finding 2MASS Positions

The initial list of positional data for the 8623 targets originates from the MSX catalog by the primary investigators using the color ranges in Table 1. The 2MASS catalog is a crucial cross-match, as the 2MASS positional accuracy is approximately 10 times better than the MSX positional accuracy. These 2MASS positions are later used in the data reduction pipeline for both the VLA and ALMA observations, improving the detection rate.

My first task was to cross-match the MSX positions to the 2MASS catalog. The 2MASS

Table 2: Catalogs used to create IR catalog for BAaDE Sources. Table includes the final count for each catalog out of the 8623 sources chosen from the MSX catalog.

| IR Catalog Selection | Central Wavelength ( $\mu\text{m}$ ) | Final Matches |
|----------------------|--------------------------------------|---------------|
| MSX All              |                                      | 8623          |
| MSX A                | 8.28                                 | 8622          |
| MSX C                | 12.13                                | 8616          |
| MSX D                | 14.65                                | 8611          |
| MSX E                | 21.34                                | 7871          |
| 2MASS All            |                                      | 7251          |
| 2MASS J              | 1.24                                 | 7250          |
| 2MASS H              | 1.66                                 | 7249          |
| 2MASS K              | 2.16                                 | 7249          |
| DENIS All            |                                      | 2410          |
| DENIS I              | 0.79                                 | 1084          |
| DENIS J              | 1.24                                 | 1750          |
| DENIS K              | 2.19                                 | 1552          |
| WISE All             |                                      | 4639          |
| WISE1                | 3.4                                  | 3811          |
| WISE2                | 4.6                                  | 3602          |
| WISE3                | 12                                   | 1517          |
| WISE4                | 22                                   | 1892          |
| GLIMPSE All          |                                      | 1386          |
| GLIMPSE1             | 3.6                                  | 949           |
| GLIMPSE2             | 4.5                                  | 669           |
| GLIMPSE3             | 5.8                                  | 1055          |
| GLIMPSE4             | 8.0                                  | 649           |
| ISOGAL All           |                                      | 328           |
| ISOGAL07             | 7                                    | 277           |
| ISOGAL15             | 15                                   | 283           |
| MIPSGAL24            | 24                                   | 1267          |
| AKARI All            |                                      | 5557          |
| AKARI09              | 9                                    | 4827          |
| AKARI18              | 18                                   | 4952          |
| HERSCHEL70           | 70                                   | 2245          |

| Catalog  | Flag                                 | Value for Exclusion  |
|----------|--------------------------------------|--|
| MSX      | Qa                                   | < 2  |
| 2MASS    | ph_flag<br>or ph_flag<br>and rd_flag | 'X'<br>'U'<br>'0' or '6'                                     |
| DENIS    | #flg<br>#qual                        | not = '0000'<br>i 80   |
| WISE     | ext_flg<br>cc_flg<br>ph_qual         | not = 0<br>not = 'O', 'D', 'P', 'H', 'o'<br>not = 'A' or 'B' |
| AKARI    | EXTENDED##<br>FQUAL##                | not = 0<br>not = 3   |
| ISOGAL   | mag#<br>qual#                        | 88.88' or '99.99'<br>< 3                                     |
| HERSCHEL | flag_edge<br>flag_blend              | not = f<br>not = 0   |
| GLIMPSE  | No flags applied.                    |  |
| MIPSGAL  | No flags applied.                    |  |

Table 3: Photometry filters used when creating IR catalog for the extended color sources.

position matches were then used to search the other catalogs, many of which had already been cross-matched with 2MASS in their respective databases. For the few sources lacking 2MASS information, the original MSX positions were used. Each MSX position was searched with a  $5''$  radius so as not to miss a possible cross-match in 2MASS. This sometimes resulted in multiple candidates per MSX position, totaling 3600 multiple matches to sort and filter to determine the best 2MASS match.

### 2.3 Photometry Filtering

Along with the initial cross-matching based on position, we filtered each catalog to remove data of poor quality. Those filters were distinct to each catalog. Examples include saturated sources, poor signal-to-noise ratios, extended sources, etc. The only exceptions are those from the Spitzer Space Telescope: GLIMPSE and MIPSGAL. These catalogs have had unreliable data removed before the final tables were published, requiring no extra filtering for our database.

## 2.4 2MASS Cases with Multiple Candidates

For those 3600 multiple matches, various criteria and filters were used to reduce the list to a one-to-one match between MSX and 2MASS. The first criteria used colors for each candidate. Comparisons were made between the same color within a multiple-matched set and color precedence was applied in the following order: J-K, J-H, H-K. In each comparison, the source with the reddest color value was kept, as the AGB sources we target are extremely red objects.

Not every candidate had detections in multiple bands, so the next criteria rejected candidates with a detection in only J-band ( $1.24 \mu\text{m}$ ), since we are looking for redder sources. Red sources detected in J-band are expected to be detected in H- and K-band ( $1.66$  and  $2.16 \mu\text{m}$ ); thus a non-detection in H and K implies a different type of source. If every candidate match was detected only in J-band, we kept the match with the highest signal-to-noise ratio (SNR) as we expect the correct targets to be very bright.

The next criteria focused on the brightest match in the K or H-band, with K being the preference. To pick the brightest candidate the magnitude had to be brighter by at least 0.2 magnitudes; otherwise we selected the match with reported coordinates closest to the search coordinates.

In some cases, the matches in a candidate set displayed a trend where one was detected in K-band only while the others were detected in J and H-band only. According to 2MASS documentation, this is a result of a failure in the band-merging process. In those cases, we kept the position with the K-band detection.

The remaining sets of multiple matches were filtered manually, either by inspection of the data or by using the IRSA online finder chart to visually inspect the sources for the reddest, brightest, and closest source to the original position.

| Catalog   | Initial Matches                          | Initial 1-to-1                           | Final Matches                            |
|-----------|--|--|--|
| 2MASS     | 9274                                     | 5639                                     | 7251                                     |
| DENIS     | 7488                                     | 2521                                     | 2410                                     |
| WISE      | 1: 3817<br>2: 3606<br>3: 1517<br>4: 1892 | 1: 3805<br>2: 3598<br>3: 1517<br>4: 1892 | 1: 3811<br>2: 3602<br>3: 1517<br>4: 1892 |
| GLIMPSE1  | 1495                                     | 927                                      | 1385                                     |
| GLIMPSE2A | 629                                      | 334                                      |  |
| GLIMPSE2B | 592                                      | 343                                      |  |
| GLIMPSE3A | 158                                      | 96                                       |  |
| GLIMPSE3B | 143                                      | 104                                      |  |
| ISOGAL    | 328                                      | 328                                      | 328                                      |
| MIPSGAL   | 1267                                     | 1267                                     | 1267                                     |
| AKARI     | 9: 4827<br>18: 4953                      | 9: 4827<br>18: 4951                      | 9: 4827<br>18: 4952                      |
| HERSCHEL  | 2246                                     | 2244                                     | 2245                                     |

Table 4: Cross matching statistics for catalogs included in the BAaDE IR database.

## 2.5 Other Catalogs with Multiple Candidates

DENIS: The DENIS catalog was the most difficult to match due to the catalog listing each detection as an independent event and does not merge detections of the same object. This causes multiple matches per 2MASS position. However, the photometry filtering process (using the flags listed in Table 2) removed a good number of multiple matches. For those left, I calculated the mean magnitude for each candidate set of matches.

GLIMPSE: The GLIMPSE catalogs gave some multiple matches to the 2MASS positions, but fortunately, the catalogs contain a 2MASS identifier field (`tmass_designation`) which was used to cross match with our 2MASS sources already identified as discussed above. This process left me with all single matches. The five GLIMPSE catalogs were combined into a single listing in the IR catalog. If a candidate was matched in multiple catalogs, the mean magnitude was reported in the IR catalog.

OTHERS: For the other catalogs, no multiple matches were left after the photometry filtering.

## 2.6 Cross-Match Confirmation with 2MASS

Due to the multiple filters applied to resolve the multiple matches between MSX and 2MASS sources, there is an expectation that at least a few incorrect matches may have been chosen. As a check to see to what extent this may have occurred, an alternate set of search coordinates were created by shifting the original search coordinates. The total offset is between  $89''$  and  $115''$  from the original. This created a pseudo-randomized positional grid which could then be used to construct a control sample not focused on the relatively rare AGB stars. We compared the colors and magnitudes of the two samples. Figure 4 shows the BAaDE and the shifted sample in a color-magnitude and color-color diagram. While there is some overlap, particularly in the iiib sources, the BAaDE sample, which is pre-selected to be red and bright sources, is clearly offset from the random sample particularly for the ii sources. This demonstrates that our filtering methods to select the candidate cross-match most likely to be a red giant worked for the ii sources. The iiib sources overlapping the random sources may be due to a selection error in the 2MASS catalog, as the iiib sources are even redder than the iiia sources and may not be visible in the shorter wavelengths of 2MASS. This will lead to some correction work with the IR catalog for these extended sources. This is explored and discussed further in Section 5.

## 3 Radio Data

### 3.1 Observations with the Very Large Array

As stars evolve off the Main Sequence and move toward the Giant Branch (as seen in Figure 1), they become surrounded by a thick circumstellar shell that redistributes much of their stellar light into the IR regime. In this shell molecules form, and the conditions are sometimes conducive to maser formation of SiO, OH, and H<sub>2</sub>O with transitions in the radio and millimeter regime. Their brightness and recognizable appearance in the radio regime makes it relatively easy to observe using telescopes such as the Very Large Array (VLA)

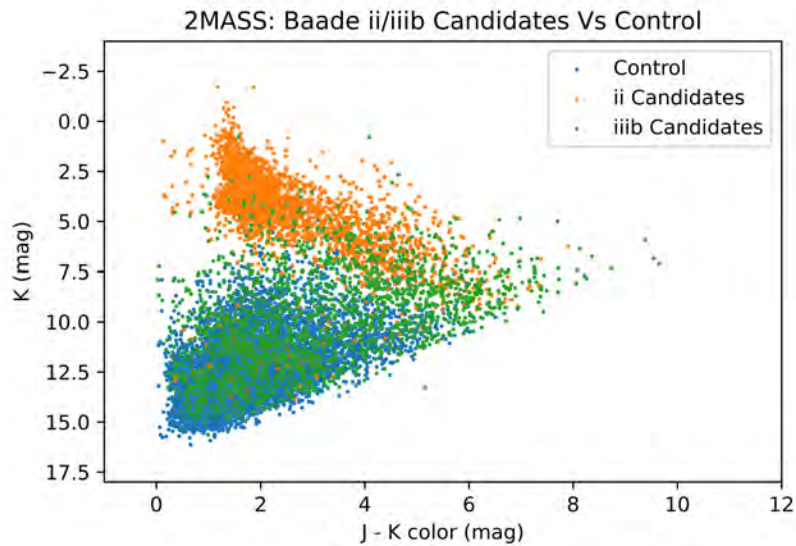


Figure 3: 2MASS source selection comparison between BAaDE selected sources and randomly selected sources in the same area of the sky. Sources were treated in the same manner with regard to photometry. The 2MASS sources cross-matched to our IR-selected region ii BAaDE sources are clearly distinct from a randomly selected sample of stars in the same region of the sky. The iiib BAaDE sources appear bluer than expected, leading to the possibility that the wrong sources were chosen in 2MASS due to the iiib region being redder and not visible in the bluer 2MASS bands. This is discussed further in Section 5.

near Socorro, New Mexico. As a blind SiO maser search would be quite time consuming due to the small beam at the frequencies of the SiO masers and thus unreasonable, we can instead use the IR properties to pre-select stars likely to harbor masers (Sjouwerman *et al.*, 2009; Messineo *et al.*, 2004) to select candidates worth observing for potential maser activity. The MSX mission has bands in the mid-IR used to identify suitable candidates (Sjouwerman *et al.*, 2009) (Table 1).

The BAaDE survey spectral setup for the VLA covers the 43 GHz J=1—0  $^{28}\text{SiO}$   $v=0$ , 1, 2, and 3 transitions, as well as the  $^{29}\text{SiO}$   $v=0$ , 1 and  $^{30}\text{SiO}$   $v=0$  transitions all of which may be detected in a different combination per source. The SiO  $v=0$  transition can be detected as either a thermal or a maser line, while the other transitions are strictly maser detections in the BAaDE data (Lewis, 2021). The only molecule identified in any of the VLA spectra is SiO due to the judicious spectral set-up chosen specifically for its coverage of SiO maser lines and a short integration time for each source also chosen to accommodate maser emission. We observed 503 out of the 8623 identified ii and iiib candidates as a test set in expanding the IR color range for investigating line ratio correlations. The observations were divided up into 13 different observational runs (each resulting data set is called a Science Data Model, or SDM). The 13 runs covered a narrow band of the sky near the Galactic center (Figure 5). The SiO maser detection rate of the 503 sources searched via the VLA is 28%.

### 3.1.1 Data Reduction

The data reduction took place using the National Radio Astronomy Observatory’s Astronomical Image Processing System (AIPS) (<http://www.aips.nrao.edu>), and utilized a pipeline developed for the original BAaDE survey. We shifted the data to the updated, more accurate 2MASS position before calibration in order to optimize the detection rate. After spectra had been formed at each target position, the spectra were searched for possible line detections using a specially developed python script.

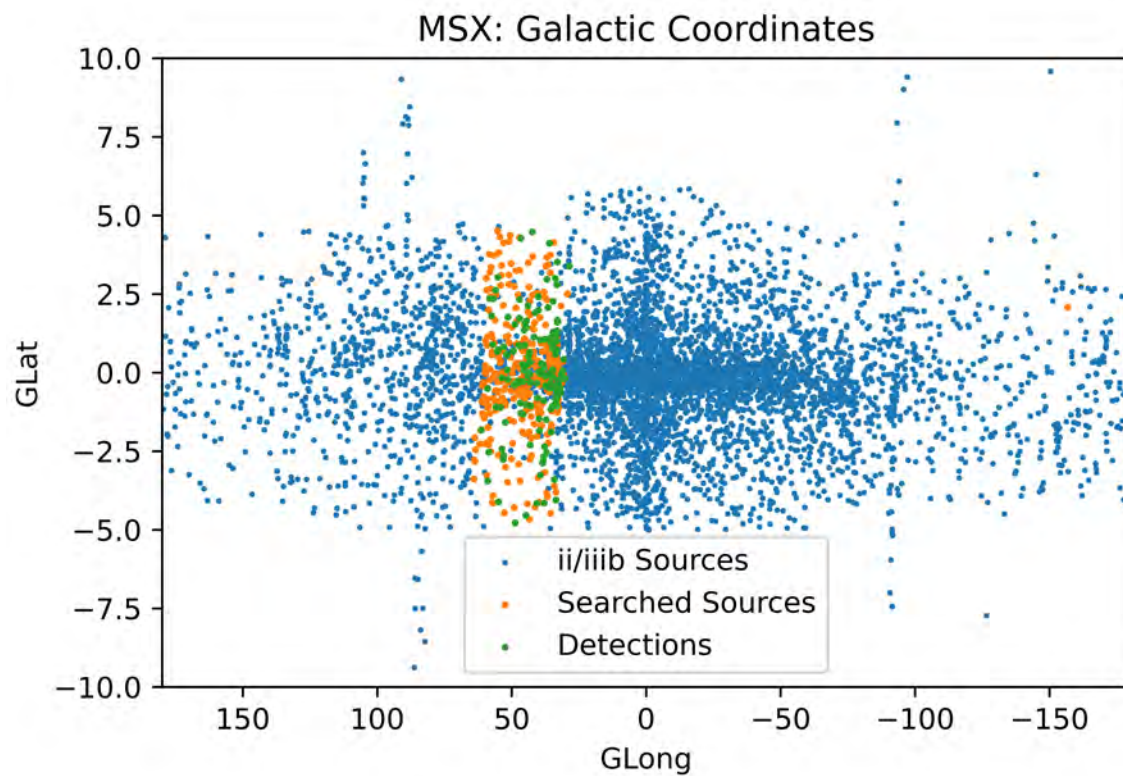


Figure 4: Plot shows where the BAaDE extended color range sources are located on the galactic plane. The orange sources were included in the VLA observations, with the green sources being detected SiO masers.

## 3.2 Results

503 sources were observed during 12 different time slots (listed by SDM in table 3). There is a 13th SDM (1738) that would not get through the software pipeline with any reliable results. Of the 12 SDMs, there were 140 detections, with a 28% detection rate. This is lower than the detection rate of the original source set which was 53.5%. We expect there to be fewer SiO masers in the ii and iiib regions due to their differing CSE properties as compared to the iiia region, and this lower detection rate matches our expectations. The original survey of sources were mostly chosen in the iiia region as the selection criteria was optimized for certain CSE conditions that harbor SiO masers. It is worth noting we only observed 503 of the 8623 sources, or just 5.8%, while there were 30,000 original 3a sources with 18,000 observed between the VLA and ALMA (60%).

A scatter plot for the  $v=1/v=2$  line ratio versus A-D color was made to investigate whether a correlation could be confirmed (Figure 7). The data represented in Figure 7 has a Pearson Correlation coefficient of -0.0086 with a p-value of 0.45. The Pearson Correlation is a parametric measure that produces a sample correlation coefficient which measures the strength and direction of linear relationship between pairs of continuous variables. A coefficient of 0 indicates there is no relationship. General guidelines require at least a 0.1 for it to be considered a small or weak correlation.

Of the 140 detected SiO masers, 41 were repeat detections from the original survey. While analyzing this set of VLA observations, it came to light that some of our sources that fit the ii and iiib criteria for certain color ranges (mainly C-E and A-E as listed in Table 1), they were also considered iiia sources in the A-D color and were thus a part of the original set of VLA observations. These detections can be seen in figures 6 and 7. While these double detections were not intentional and did not extend the search for correlations as it did not extend the color range as much as we had hoped, this does lead to further research possibilities as we now have another epoch for these 41 masers.

| SDM    | Total   | ad2i  | ad3b  | ae2i   | ae3b | ce2i  | ce3b  |
|--------|---------|-------|-------|--------|------|-------|-------|
| 1737   | 18/47   | 0/13  | 6/11  | 4/7    | 1/6  | 3/3   | 4/7   |
| 1739   | 20/46   | 0/8   | 6/11  | 4/9    | 1/3  | 6/10  | 3/5   |
| 1740   | 16/46   | 1/14  | 7/9   | 4/10   | 2/7  | 2/5   | 0/1   |
| 1741   | 17/46   | 2/21  | 7/8   | 5/11   | 0/1  | 1/2   | 2/3   |
| 1742   | 8/40    | 0/17  | 3/6   | 3/10   | 0/2  | 2/4   | 0/1   |
| 1743   | 7/40    | 1/23  | 0/4   | 3/7    | 1/3  | 1/1   | 1/2   |
| 1744   | 9/40    | 1/23  | 3/6   | 4/8    | 0/0  | 1/2   | 0/1   |
| 1745   | 9/39    | 1/17  | 1/6   | 2/5    | 1/5  | 1/1   | 3/5   |
| 1746   | 6/40    | 1/18  | 2/5   | 2/12   | 0/3  | 1/1   | 0/1   |
| 1747   | 11/40   | 0/15  | 4/5   | 4/10   | 0/5  | 0/0   | 3/5   |
| 1748   | 6/40    | 0/22  | 4/9   | 1/2    | 0/3  | 0/1   | 1/3   |
| 1749   | 13/39   | 1/15  | 1/5   | 5/12   | 1/2  | 1/1   | 4/4   |
| Totals | 140/503 | 8/206 | 44/85 | 41/103 | 7/40 | 19/31 | 21/38 |
|        | 28%     | 4%    | 52%   | 40%    | 18%  | 61%   | 55%   |

Table 5: List of SDMs and their detection rates, broken down by the source names which were names based on their selection criteria and region ii or iiib. Each column per name represents the number of detections versus the number of sources searched with that naming convention.

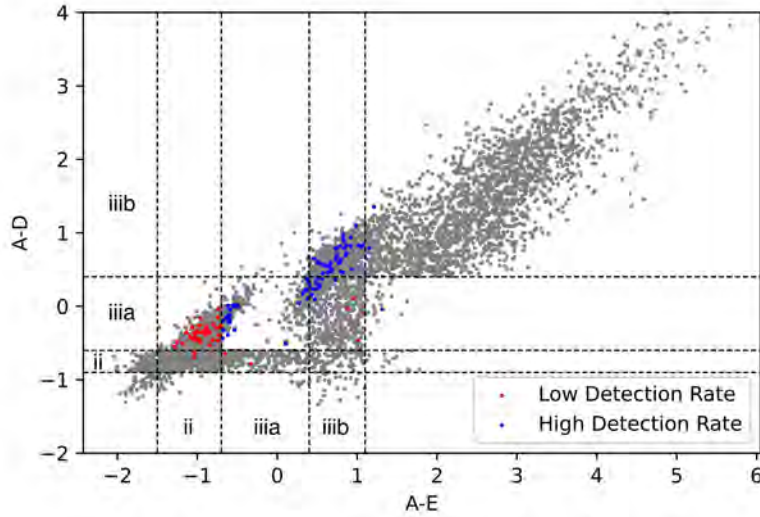


Figure 5: MSX color data plotted in grey. High and low detection rates are based on Table 4's breakdown of the types of sources searched. The ad3b, ce2i, ce3b sources had higher rates of maser detection ( $> 50\%$ ) than the ad2i, ae2i, and ae3b sources. The ce2i sources are the blue dots in the iiia region of the plot, also detected in the original survey as ad3a's. The dashed lines represent the color ranges as listed in Table 2.

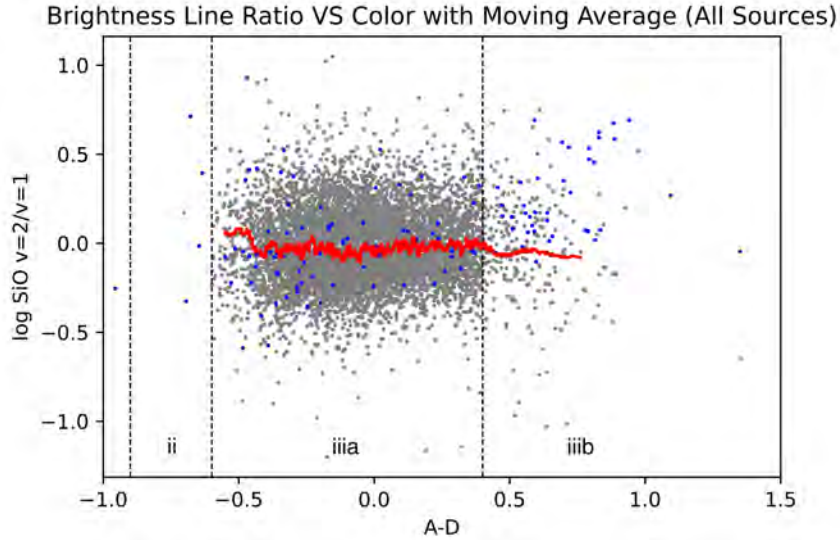


Figure 6: A-D color plot versus SiO  $v=1/v=2$  line ratios. The grey sources are the original iiia sources, while the blue sources were chosen with the intention to extend the color range. Many of those chosen for this extended color range actually fell into the iiia color range as well. The dashed lines represent the color ranges as listed in Table 2.

## 4 Discussion

### 4.1 Overall detection trends

Looking at Table 5’s detection breakdown by color, we achieved very few detections in the ii sources, which likely is due to the CSEs being too thin, not sustaining maser emission buildup. Higher detection rates is seen in the iiib sources, which still are dense enough to sustain maser emission. The targets in the ii region had a detection rate of 20% while the targets in the iiib region had a detection rate of 44%. For the very reddest sources we do not see masers; a likely reason for this is that as the shell gets denser there will be more and more collisions de-exciting the molecules, hence ‘quenching’ the maser process.

### 4.2 Line Ratios Versus Infrared Color

In 2007, Nakashima and Deguchi Nakashima & Deguchi (2007) published a study of 75 SiO masers with a correlation between infrared colors and intensity ratios when using IRAS

flux densities with wavelengths of 25 and 12  $\mu\text{m}$ , MSX E and C bands, and 2MASS H and K bands. They used velocity-integrated intensities rather than peak intensities, the paper mentions the two intensities give similar results. Stroh, et al. (Stroh, 2019) compared these two intensities as well for the BAaDE sources and concluded there was not enough difference in the results to require the extra step of calculating the velocity-integrated intensities. Peak intensities were used in both the original line ratio results by Lewis, (2021) and in these extended color range results. So while there are different ways to measure line ratios, it does not appear to be a reason for the discrepancy between different investigators' results.

To investigate whether the previously reported correlation between CSE color and SiO line ratio holds, I plotted the SiO  $v=2/v=1$  line ratio as a function of A-D color in Figure 7. As can be noted, there is a large scatter in the line ratio values, making it difficult to discern a trend. The red line is a moving average of the line ratio values, also not displaying a visible trend. No significant correlations are found between any SiO line ratios and any IR color in either the original sample (Lewis, 2021) or the expanded color range sample as shown in Figure 7. As mentioned in the Results section, this was also tested statistically with a Pearson correlation test, giving a coefficient of -0.0086 with a p-value of 0.45. This implies that whatever is supporting the  $v=1$  line is equally good in supporting the  $v=2$  line.

In figures 8 and 9, the left is from Nakashima and Deguchi's findings with their 75 masers (Nakashima & Deguchi, 2007) while the right is my re-creation using our 140 maser detections. The left shows a much sharper slope, indicating a higher correlation while Figure 9 shows a moving average with no obvious linear correlation. The data represented in Figure 9 has a Pearson Correlation coefficient of -0.0086 with a p-value of 0.9.

The  $^{28}\text{SiO}$   $v=1$  and  $v=2$  lines are the primary maser lines in BAaDE's spectral setup and are almost always detected as a pair. These lines are usually the brightest in a given source and as such are nearly always present when any additional lines are detected, other than the  $v=0$  thermal line (Lewis, 2021). The  $^{28}\text{SiO}$   $v=3$  line is considerably fainter than the  $v=1$  or  $v=2$  lines, though sources with all 3 lines are hosting generally brighter masers

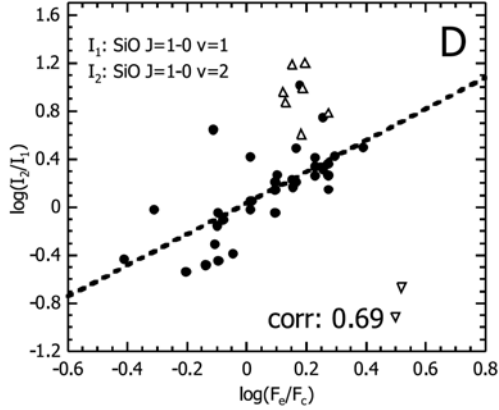


Figure 7: Plot from (Nakashima & Deguchi, 2007) 2007 paper showing a significant correlation between color and line ratios.

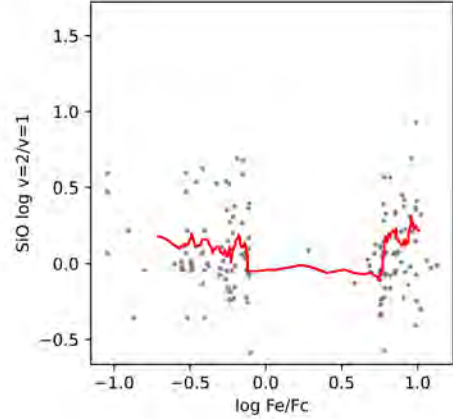


Figure 8: Recreation of (Nakashima & Deguchi, 2007)'s plot using our VLA observations and IR data for the ii and iiib sources. Red line is a moving average. No significant correlation found.

than sources with only  $v=1$  and  $2$ . While I am reporting here on the ratio of  $v=2/v=1$  lines, I also investigated other line ratios using  $v=3$  and  $v=0$ , though none showed correlations with IR color, similar to the results reported in this paper. Rather than line ratios, I also investigated line strengths as a function of color but also saw no correlations.

Some models show that the  $v=0$  lines preferentially form in thinner shells while the  $v=3$  lines may be more common in thicker shells (Desmurs *et al.*, 2014). Desmurs, *et al.* (2014) suggests that the  $v=2/v=1$  line ratio may trace the density in the circumstellar envelope with SiO  $v=1,2,3$  maser emission peaking at successively higher densities. The denser circumstellar shells are found to have redder infrared emission such as those described by the color range in region iiib of Figure 2, and may include the densities required for the brighter  $v=2$  line. With the expanded data, it is still unclear if there is any relation between line ratios and IR color.

There are two distinct possibilities for why previous work has reported different results. First, previous work had small sample sizes. Looking at Nakashima and Deguchi's work (Figure 8) (2007) their sample size only contained 75 SiO masers, while the extended color

range reported here had 140, and then the original color range (Lewis, 2021) had nearly 10000 SiO maser detections. It seems that as the data set grows, any correlation seems to wash out. Second, the AGB target stars are varying with time. The IR radiation varies, causing changes in the A-D color. The amplification of masers is exponential and also varies with time. We cannot separate our data as a function of stellar phase and thus we cannot account for the varying IR radiation and maser emission.

## 5 Future Work

There are some unresolved issues that would require more time to investigate. The VLA pipeline relies heavily on 2MASS positions for our target sources as the 2MASS catalog has a higher resolution than the MSX catalog. This caused an issue with the extended iiib sources as they are redder than the original iiaa sources and as such may not be detectable in the 2MASS J,H,K bands. When the new 8600 sources are plotted with 2MASS data (K vs J-K band), many of the iiib sources show up as bluer on the plots despite their being chosen as redder sources (Figure 9). I also looked at a distribution of how far away the 2MASS selected position compares to the original MSX position. As discussed previously, I used a radius of 5 arcsec when searching other catalogs. Looking at Figure 10, the ii targets' 2MASS positions are for the most part close to the MSX position, while the iiib targets' positions are more evenly distributed throughout the 5 " search radius, indicating that the position and photometry data is not originating from the AGB source we are observing.

A magnitude/color cut was chosen to remove the 2MASS data that I assume is the wrong sources for the chosen MSX positions. This cut removed 2389 iiib sources' 2MASS data ( half of the total iiib sources). The VLA data was then re-run through the NRAO AIPS pipeline without these 2MASS positions for those 2389 iiib sources. Figure 11 shows the changes in SiO maser detections. When re-running the pipeline after the magnitude/color cut, there was an overall gain of just 3 detections, with a total of 143 (as compared to the 140 discussed previously).

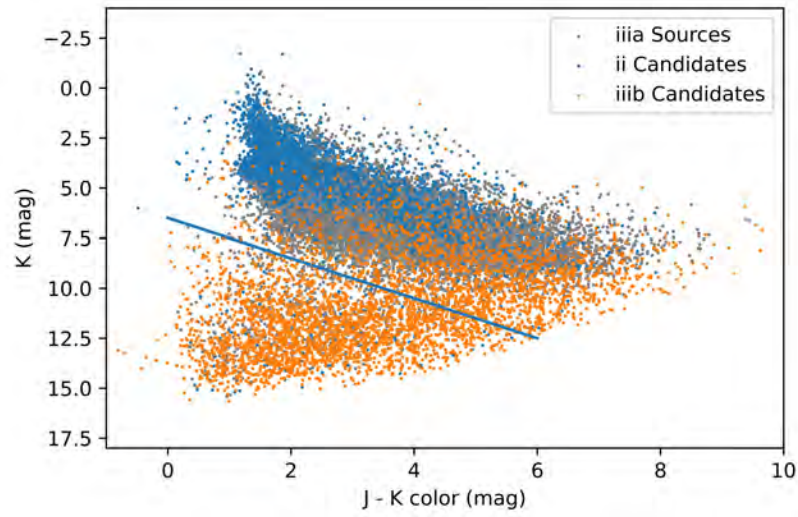


Figure 9: Similar to Figure 4, only now showing the magnitude/color cut made to remove possible incorrect 2MASS data due to the iiib sources being too red for detection in the 2MASS bands.

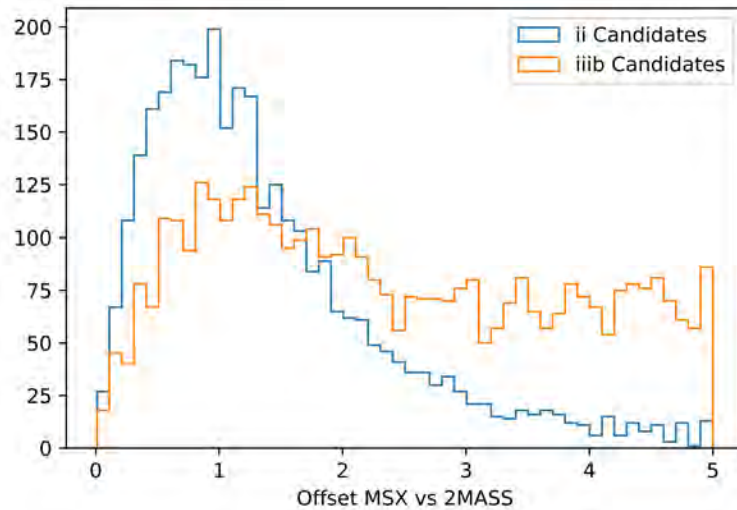


Figure 10: Histogram showing the 2MASS positions' offset as compared to the MSX search position. While the ii sources were mostly close (within 2 ") of the original position, the iiib sources have larger offsets, indicating that perhaps the correct 2MASS data source was not chosen.

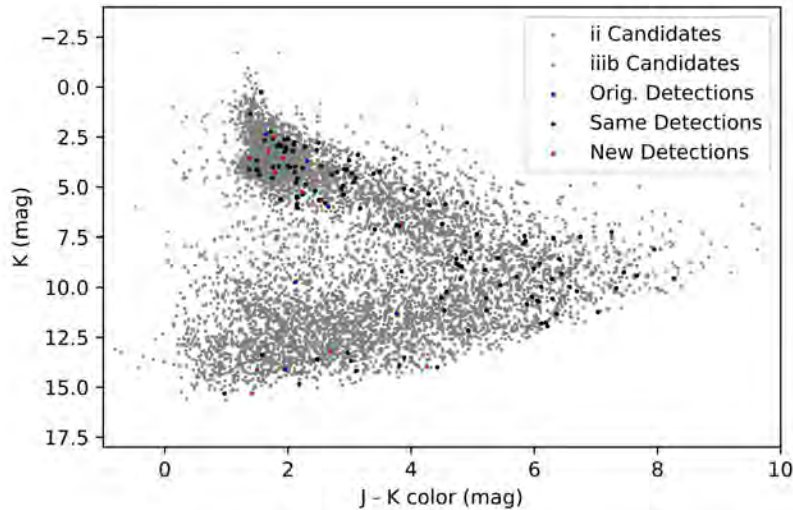


Figure 11: The grey dots represent all of the ii and iiib sources that had J and K data from 2MASS. Blue dots represent detections that were found during the first pipeline run-through but not the second. Red dots represent new detections found in the second run-through but not the first. The black dots remain changed between different pipeline runs.

There was a significant change of detections in the ii region, which was surprising given that the applied magnitude/color cut and resulting loss of 2MASS positions were not changed for these region-ii targets. Due to the brightness of masers, the maser detections themselves are used for calibration. This works best when there is a high detection rate. Given the original detection rate of just 28%, this calibration method may not be sufficient enough to catch all of the possible masers in the observations by the VLA. Since we are focused on the central part of the Milky Way, the field is often crowded and many of the targets are very close (within a few arcseconds) to one another. It is possible that by changing the iiib positions back to their MSX positions, it may have affected close-by region-ii detections. This is something that could be explored further to ensure we find all possible masers in the observations.

## 6 Conclusion

There are several possible explanations for the lack of correlation between line ratios and IR color. First, the BAaDE spectra and IR data were not taken simultaneously. As the BAaDE sources are primarily variable AGB stars, source photometry reported by the various IR surveys might not be taken at the same stellar phase as the BAaDE observations from the VLA. Second, even though we attempted to expand the narrow color range of the original survey, there was some overlap in target sources (41 extended color targets were also included in the original target list) meaning the expanded set was not as independent nor as expanded as we would have liked. The narrow color range makes it difficult to detect a weaker correlation. Third, none of the sources have been reddening-corrected. We do not have reliable distances for a statistically significant portion of our sample and therefore all colors are presented as observed with no reddening corrections.

While none of these explanations are strong issues on their own, the combination of drivers behind the lack of correlation is significant, particularly since other, smaller samples have shown stronger correlation between line ratios and color (eg., (Nakashima & Deguchi, 2007)). It is thought that both SiO line ratios and IR colors would trace conditions of the circumstellar shell, so this result may simply be shining light on the idea that the IR-SiO line correlation is highly dependent on stellar phase. Other comparisons may be necessary to disentangle which CSE properties affect the line ratios, such as looking at more direct physical measurements like mass-loss rate, luminosity, density, and temperature Lewis (2021).

## 7 Acknowledgements

I would like to thank Ylva Pihlström for her guidance, expertise, and support as well as for being a model mentor and researcher. I would also like to thank all those on the BAaDE team for their work that help to support this thesis, including Megan Lewis, Loránt Sjouwerman, Eddie Hilburn, and Michael Stroh.

This research makes use of data products from the Two Micron All Sky Survey, which is a joint project of the University of Massachusetts and the Infrared Processing and Analysis Center/California Institute of Technology, funded by the National Aeronautics and Space Administration and the National Science Foundation.

This research has made use of the NASA/ IPAC Infrared Science Archive, which is operated by the Jet Propulsion Laboratory, California Institute of Technology, under contract with the National Aeronautics and Space Administration.

This publication makes use of data products from the Wide-field Infrared Survey Explorer, which is a joint project of the University of California, Los Angeles, and the Jet Propulsion Laboratory/California Institute of Technology, and NEOWISE, which is a project of the Jet Propulsion Laboratory/California Institute of Technology. WISE and NEOWISE are funded by the National Aeronautics and Space Administration.

Herschel is an ESA space observatory with science instruments provided by European-led Principal Investigator consortia and with important participation from NASA.

This research is based [in part] on observations made with the Spitzer Space Telescope, which is operated by the Jet Propulsion Laboratory, California Institute of Technology under a contract with NASA.

This publication makes use of data products from the Two Micron All Sky Survey, which is a joint project of the University of Massachusetts and the Infrared Processing and Analysis Center/California Institute of Technology, funded by the National Aeronautics and Space Administration and the National Science Foundation.

This research is based on observations with AKARI, a JAXA project with the participation of ESA.

## References

Desmurs, J. F., Bujarrabal, V., Lindqvist, M., Alcolea, J., Soria-Ruiz, R., & Bergman, P.

2014. SiO masers from AGB stars in the vibrationally excited  $v = 1$ ,  $v = 2$ , and  $v = 3$  states. , **565**(May), A127.
- Habing, H. J. 2016. Orbits of maser stars in the rotating Galactic bar. , **587**(Mar.), A140.
- Hilburn, Eddie. 2018. Infrared Properties of Stars in the Bulge Asymmetries and Dynamical Evolution Survey.
- Lewis, Megan. 2021. Probing the Galactic AGB population through infrared and SiO maser emission.
- Messineo, M., Habing, H. J., Menten, K. M., Omont, A., & Sjouwerman, L. O. 2004. 86 GHz SiO maser survey of late-type stars in the inner Galaxy. II. Infrared photometry of the SiO target stars. , **418**(Apr.), 103–116.
- Nakashima, Jun-ichi, & Deguchi, Shuji. 2007 (Mar.). SiO maser observations of a wide dust-temperature range sample. *Pages 266–270 of: Chapman, Jessica M., & Baan, Willem A. (eds), Astrophysical Masers and their Environments*, vol. 242.
- Sjouwerman, Loránt O., Capen, Stephanie M., & Claussen, Mark J. 2009. Midcourse Space Experiment Versus IRAS Two-Color Diagrams and the Circumstellar Envelope-Sequence of Oxygen-Rich Late-Type Stars. , **705**(2), 1554–1565.
- Stroh, Michael. 2019. Circumstellar SiO Masers in the Bulge Asymmetries and Dynamical Evolution Survey.
- Stroh, Michael C., Pihlström, Ylva M., Sjouwerman, Loránt O., Lewis, Megan O., Claussen, Mark J., Morris, Mark R., & Rich, R. Michael. 2019. The Bulge Asymmetries and Dynamical Evolution (BAaDE) SiO Maser Survey at 86 GHz with ALMA. , **244**(2), 25.